THE ASTRONOMICAL JOURNAL, 118:2675–2688, 1999 December

THE RISE TIME OF NEARBY TYPE Ia SUPERNOVAE

ADAM G. RIESS,[1] ALEXEI V. FILIPPENKO,[1] WEIDONG LI,[1] RICHARD R. TREFFERS,[1] BRIAN P. SCHMIDT,[2] YULEI QIU,[3] JINGYAO HU,[3] MARK ARMSTRONG,[4] CHUCK FARANDA,[5] ERIC THOUVENOT,[6] AND CHRISTIAN BUIL[6]

Received 1999 July 12; accepted 1999 August 24

ABSTRACT

We present calibrated photometric measurements of the earliest detections of nearby Type Ia supernovae (SNe Ia). The set of ~ 30 new, unfiltered CCD observations delineate the early rise behavior of SNe Ia 18 to 10 days before maximum. Using simple empirical models, we demonstrate the strong correlation between the rise time (i.e., the time between explosion and maximum), the postrise light-curve shape, and the peak luminosity. Using a variety of light-curve shape methods, we find the rise time to B maximum for an SN Ia with $\Delta m_{15}(B) = 1.1$ mag and peak $M_V = -19.45$ mag to be 19.5 ± 0.2 days. We find that the peak brightness of SNe Ia is correlated with their rise time; SNe Ia that are 0.10 mag brighter at peak in the B band require 0.80 ± 0.05 days longer to reach maximum light. We determine the effects of several possible sources of systematic errors, but none of these significantly impacts the inferred rise time. We explore the degree to which comparisons between the observed and theoretically predicted rise times constrain SN Ia progenitor systems.

Key words: cosmology: observations — supernovae: general

1. INTRODUCTION

A few weeks after explosion, the visual luminosity of a Type Ia supernova (SN Ia) increases a trillionfold, by which time its peak output can rival the glow of its host galaxy. Unfortunately, this dramatic rise to prominence is difficult to detect and therefore remains poorly documented (Vacca & Leibundgut 1996; Leibundgut et al. 1991a, 1991b). Enough of this rise occurs in the first few hours after explosion that it is possible to detect low-redshift ($z < 0.02$) SNe Ia that are less than 1 day old.

Discovering SNe Ia in their youth requires great persistence and good fortune; potential host galaxies must be monitored frequently to increase the odds of an early detection. Even when SNe Ia are detected early in their development, the observations are often recorded with a medium that does not easily lend itself to precise, quantitative analysis: naked-eye observations, photographic plate images, and unfiltered CCD images. To facilitate comparisons with subsequent observations, early SN Ia observations need to be reliably calibrated on standard passband systems using linear detectors.

To date, the earliest reliable and precisely quantifiable detection (i.e., employing a CCD and a standard passband) of a nearby SN Ia is ~ 13 days before B-band maximum, but still ~ 1 week after explosion (SN 1994D, Richmond et al. 1995). Detections of SNe Ia earlier than 10 days before B maximum have been reliably measured and reported for only four nearby SNe Ia (SN 1994ae, Riess et al. 1999b; SN 1994D, Richmond et al. 1995; SN 1992bc, Hamuy et al. 1996a; SN 1990N, Lira et al. 1998, Leibundgut et al. 1991a). This is unfortunate, as the SN Ia rise to glory during the time interval between explosion and maximum brightness (hereafter referred to as the "rise time") holds significant clues for understanding the progenitors and physics of SNe Ia (Leibundgut & Pinto 1992) and ultimately their utility for the determination of cosmological parameters.

1.1. *A Constraint on SN Ia Progenitors*

Precise knowledge of the SN Ia rise time could provide valuable constraints on models of SN Ia progenitors. Although the ways the explosion characteristics influence the SN Ia rise behavior are complex, requiring detailed simulations to understand, some general dependences can be understood.

The rise behavior of an SN Ia is determined by the rate at which energy in the interior is released and subsequently diffuses to the surface of the supernova. Although the energy deposition rate is always decreasing, homologous expansion of material continually increases the rate at which energy diffuses to the surface during the rising phase. At this epoch, the photosphere grows in radius while receding through the expanding ejecta.

The available energy source is the radioactive ^{56}Ni (followed by radioactive ^{56}Co), which is synthesized in the explosive burning of carbon and oxygen to nuclear statistical equilibrium (Hoyle & Fowler 1960; Arnett 1969; Colgate & McKee 1969; Arnett 1982; Höflich, Khokhlov, & Müller 1992; Leibundgut & Pinto 1992; Pinto & Eastman 2000). The initial progenitor mass plays an important role, providing both the source of fuel and the obstruction to energy diffusion. The rate of diffusion to the surface depends on the proximity of the radioactive material to the photosphere, the temperature, and the density of the homologously expanding envelope, factors that determine the opacity of the supernova.

Detailed modeling of the explosion yields predictions of the dependence of the progenitor initial conditions and explosion mechanism on the SN Ia rise time (Höflich & Khokhlov 1996; Höflich, Wheeler, & Thielemann 1998). In general, single white dwarf progenitor systems seem to produce the shortest rise times. The rise time of double degenerate systems is extended by the additional barrier to

[1] Department of Astronomy, University of California, Berkeley, Berkeley, CA 94720-3411.
[2] Mount Stromlo and Siding Spring Observatories, Australian National University, Private Bag, Weston Creek, ACT 2611, Australia.
[3] Beijing Astronomical Observatory, Chinese Academy of Sciences, Beijing 100080, China.
[4] UK Supernova Patrol, British Astronomical Association, Rolvenden, England, UK.
[5] 7860 NW 53 Court, Lauderhill, FL 33351.
[6] Centre National d'Etudes Spatiale des Rayonnements, 18 Avenue Edouard Belin, Toulouse Cedex 4, F-31401, France.

diffusion presented by the thick disk of the tidally disrupted companion. Among single degenerate systems with a mixture of deflagration and detonation burning fronts, explosions with larger fractions of supersonic burning produce shorter rise times (Höflich & Khokhlov 1996).

1.2. *A Theoretical Calibration of SN Ia Luminosity*

Knowledge of the SN Ia rise time also provides the means to calibrate the peak luminosity of SNe Ia independent of the Cepheid distance scale. One method is to use the rise time to indicate the instantaneous rate of energy deposition from the radioactive decay of ^{56}Ni and ^{56}Co. This method still relies on theoretical modeling to indicate the likely mass of decaying nickel and the relation at maximum between the energy deposited and that radiated (once known as Arnett's law; Arnett 1982; Arnett, Branch, & Wheeler 1985). An alternate route is to use the rise time to calibrate the luminosity of the expanding SN Ia photosphere at peak. This method also has theoretical input in the form of a spectral synthesis model. A comparison of the model and observed spectrum at peak luminosity yields the velocity of the photosphere and its model temperature. Together with the rise time, this information yields the size of the photosphere and hence the luminosity of the supernova at maximum. Although both methods are only semi-empirical, each is essentially independent, relying on a different aspect of SN Ia theoretical modeling. To be consistent, the two methods require a rise time to bolometric peak of 14 to 22 days (Nugent et al. 1995).

Because measurements of the rise time provide a new window into the physics of SNe Ia, a comparison of the rise time for high-redshift and low-redshift SNe Ia could be a valuable test of evolution. Such a comparison is performed by Riess et al. (1999a).

Here we report calibrated measurements of the earliest detections of low-redshift SNe Ia and the rise time inferred from them. These observations, beginning fewer than 2 days after the explosion, provide new constraints on SN Ia evolution, progenitors, and luminosity. As discussed in § 2, we have collected the earliest CCD images of SNe Ia. These images are usually unfiltered, and we have transformed them to standard passbands. We analyze the SN Ia rise behavior in § 3. In § 4, we explore and analyze possible systematic errors and biases in our measurements. We discuss the implications for SN Ia physics and progenitors in § 5.

2. OBSERVATIONS

2.1. *Sample Selection*

To measure the SN Ia rise behavior, we have collected the earliest available CCD images of SNe Ia. To compile our sample of observations of young SNe Ia the following selection criteria were used:

1. SNe Ia with well-sampled CCD light curves;
2. SNe Ia whose hosts were observed with CCDs between 10 and 25 days before B maximum;
3. Spectroscopically normal SNe Ia (Branch, Fisher, & Nugent 1993);
4. SNe Ia with redshift $z \leq 0.02$.

We limited our analysis to CCD observations because of their well-known advantages: they are highly linear detectors over a large dynamic range and their digital output allows us to accurately subtract contamination from underlying host-galaxy light. Criterion 1 was necessary to be able to accurately determine the date of B maximum and therefore the age of all observations. Criterion 2 targets the observations of SNe Ia that will yield the most useful constraints on the rise behavior. The period earlier than 10 days before B maximum was chosen because this is the epoch where exceedingly few SNe Ia have been observed and where new data are needed (see § 1). Criterion 3 was chosen so that the inferred rise behavior will be representative of prototypical SNe Ia. Peculiar SNe Ia have been shown to deviate substantially from linear relations derived from typical SNe Ia. This requirement can and should be relaxed in the future when a sizeable sample of very early observations of peculiar SNe Ia has been collected. Criterion 4, that the SNe Ia be nearby, is important so that observations at very early times can yield significant constraints. For example, at $z = 0.02$ an SN Ia at $\sim$15 days before B maximum will have an apparent brightness of $\sim$18.5 mag in B. This also results in a measured rise behavior that is representative of SNe Ia at low redshifts, a desirable characteristic for the comparison with the rise behavior of SNe Ia at high redshift (Goldhaber 1998; Groom 1998; Goldhaber et al. 1999; Nugent 1998).

Very early detections of supernovae are most common in supernova searches that monitor potential host galaxies with high frequency. An additional requirement is that past observations are catalogued and stored so that images of host galaxies obtained before SN discoveries can be retrieved for later analysis. In most cases, SN light in very early images is not recognized until later, when the SN brightens.

Two prolific discoverers of supernovae are the Beijing Astronomical Observatory (BAO) Supernova Search, employing a 0.6 m telescope (Li et al. 1996), and the Lick Observatory Supernova Search (LOSS), with the 0.75 m Katzman Automatic Imaging Telescope (KAIT; Treffers et al. 1997; see also Richmond, Treffers, & Filippenko 1993). The BAO search has been operating since 1996 April and to date has discovered 13 SNe Ia. LOSS has been underway since the end of 1997 and to date has discovered 14 SNe Ia.

For all SNe Ia known to pass criteria 1, 3, and 4, we queried the BAO and LOSS databases and obtained all host-galaxy images expected to be between 10 and 25 days before the observed B maxima. These observations are listed in Table 1 and include SNe 1996bo, 1996bv, 1996by, 1997bq, 1998bu, 1998dh, and 1998ef.

We also combed the IAU Circulars and an amateur supernova finders' network, VSNET,[7] for reports of very early observations of SNe Ia that also passed criteria 1, 3, and 4. This search yielded two valuable additions: SN 1998aq and SN 1990N. In addition, a prediscovery detection of SN 1998bu in NGC 3368 (M96) was reported on VSNET by amateur astronomer C. Faranda, using an unfiltered CCD and 0.25 m telescope, from his backyard in Lauderhill, Florida. This nearby SN Ia was discovered approximately 9 days before B maximum, but the image by Faranda was obtained 16 to 17 days before B maximum (Meikle & Hernandez 1999). NGC 3368 was also observed by LOSS 4 days earlier (i.e., 20 to 21 days before B maximum), though SN 1998bu was not detected. SN 1998aq was discovered by M. Armstrong (Armstrong et al. 1998), with a 0.26 m reflector and an unfiltered CCD in the

[7] Accessible at http://www.kusastro.kyoto-u.ac.jp/vsnet/SNe/SNe.html.

TABLE 1

SN Ia Early Detections

SN Ia	z	Julian Date (2,440,000 +)[a] Discovery	B_{max}	Observed	Filter	Source
1990N[a]	0.003	8,065	8,082	8,065–8,072	Unfiltered	E. Thouvenot
1994D	0.001	9,419	9,432	9,420, 9,421	B, V	Richmond et al. 1995
1996bo	0.017	10,379[b]	10,386	10,375	V	BAO
1996bv	0.017	10,400[c]	10,404	10,390	Unfiltered	BAO
1996by	0.014	10,432	10,441	10,432, 10,429	Unfiltered	BAO
1997bq	0.009	10,546	10,556	10,541	Unfiltered	BAO
1998aq	0.004	10,916	10,931	10,910, 10,916	Unfiltered	M. Armstrong
1998bu	0.003	10,943	10,952	10,932, 10,936	Unfiltered	LOSS, C. Faranda
1998dh	0.009	11,018	11,028	11,010, 11,014, 11,018	Unfiltered	LOSS
1998ef	0.018	11,104	11,114	11,096, 111,00, 11,104	Unfiltered	LOSS

[a] Also on JD 2,448,071 and 2,448,072 with B,V by Lira et al. 1998.
[b] Date of independent discovery by Armstrong et al. 1998.
[c] Date of discovery (W. D. Li 1998, private communication).

course of the UK Supernova Patrol, approximately 15 days before B maximum, and the host galaxy was also imaged $\sim$21 days before B maximum. SN 1990N was discovered by E. Thouvenot (Maury et al. 1990), using a 0.6 m telescope and an unfiltered CCD, about 17 days before B maximum and was subsequently observed with the same equipment for the next 7 days. In all cases, the observers furnished us with their unfiltered CCD images (see Table 1).

We have included SN 1994D, using the observations by Richmond et al. (1995) in B and V commencing $\sim$13 days before B maximum. Although SN 1994ae was observed in R about 13 days before B maximum by the Leuschner Observatory Supernova Search (the predecessor to the Lick search; Van Dyk et al. 1994), Ho et al. (1999) have found that the Leuschner R passband is a poor match to Johnson-Cousins R, and its transmission function has not been adequately quantified. Hence we have not included SN 1994ae in the present analysis. In § 4, we address possible biases on the rise-time measurements attributable to our sample selection.

A remarkably early detection of SN 1989B was reported by Marvin & Perlmutter (1989) on behalf of the Berkeley Automated Supernova Search 17 to 18 days before B maximum at approximately mag 17. Unfortunately, the high surface brightness of the knotty spiral arm ($R = 15.6$ in a 7.″4 aperture at the position of the SN; Wells et al. 1994) makes it extremely difficult to evaluate the brightness of a $\sim$17 mag stellar object without the aid of sophisticated galaxy subtraction procedures. Our inability to obtain this CCD image forces us to regard this early detection as merely anecdotal.

We note that several very early photographic SN Ia detections have also been reported. One detection in this category was presented by Barbon et al. (1982) for SN 1979B in NGC 3913. A prediscovery photographic plate revealed the supernova at 4.5 to 5.5 mag below peak about 14 to 18 days before maximum. The precision of this measurement is limited by the poor sampling of the light curve and the difficulty in evaluating the accuracy of the photographic magnitudes. In the course of monitoring SN 1980N in NGC 1316, Hamuy et al. (1991) obtained prediscovery photographic images of SN 1981D at 15 to 16 days before maximum. Although they report the SN to have been 5 to 6 mag below peak at this epoch, their inability to reliably subtract the galaxy background ($\sim$3 mag brighter than the SN) makes this measurement difficult to interpret. These data (and others like it) fail our selection criteria and have not been included in our analysis.

2.2. *Photometric Calibrations*

Several amateur and professional supernova searches use unfiltered CCDs to increase their efficiency: an unfiltered CCD image can reach fainter magnitudes in less time than a filtered CCD.

Of the $\sim$30 observations made approximately 10 or more days before B maximum, over 80% of the unique temporal samplings of the early rise are recorded with unfiltered CCDs. The images that employed standard filters were obtained at the oldest ages of our sample (10 to 13 days before B maximum) and yield the weakest constraints on the rise behavior.

If we wish to quantify the behavior of SNe Ia at the earliest observed times we need to make use of the available unfiltered CCD observations of young SNe Ia. By either empirically characterizing a CCD's sensitivity or with explicit knowledge of its response function, it is possible to accurately transform an unfiltered SN Ia magnitude to a standard passband for comparison with subsequent filtered observations. The same method has been used by Schmidt et al. (1998) to transform supernova magnitudes observed with nonstandard filters to a standard system. Here we will review the steps in the transformation. In what follows, we will consider the standard passband to be Johnson V, but this transformation process is general and valid for other passbands.

We first measured the differences in the unfiltered magnitudes between the SNe and individual local standard (LS) stars in the SN fields. In cases with significant host-galaxy light at the position of the SN, we initially subtracted template images of the host galaxy and then fitted point-spread functions to the SN and LS stars (Schmidt et al. 1998).

Referring to an individual, unfiltered CCD system as a nonstandard passband system called "W" (for white light), the result is the measured quantity

$$\Delta W = W_{SN} - W_{LS} , \quad (1)$$

or the magnitude difference between the SN and any LS star in the W passband.

On photometric nights at each of the telescopes, Landolt (1992) standard fields were observed to derive transformations between instrumental and expected magnitudes. These transformations were used to calibrate Johnson B and V passband magnitudes and colors of the LS stars.

Now we seek a transformation of the LS stars from the standard passband, in this case V, to the nonstandard, W. This transformation is simply the pseudocolor $V-W$ for any LS star. If we know the spectral energy distribution (SED) of a LS star, this pseudocolor is

$$V-W = -2.5 \log \left[\frac{\int S_V(\lambda) F_\lambda(\lambda) d\lambda \int S_W(\lambda) d\lambda}{\int S_W(\lambda) F_\lambda(\lambda) d\lambda \int S_V(\lambda) d\lambda} \right] + \mathrm{ZP}_V - \mathrm{ZP}_W , \quad (2)$$

where $F_\lambda(\lambda)$ is the spectrum of a LS star in units of power per unit area per unit wavelength, ZP_V and ZP_W are the zero points of the V and W filter systems,[8] and $S_V(\lambda)$ and $S_W(\lambda)$ are the dimensionless sensitivity functions of the V and W systems. We refer to $V-W$, as defined by equation (2), as a "pseudocolor" because the sensitivity functions of the V and W bands generally have much more overlap than do the passbands in most standard systems.

For each observatory's $S_W(\lambda)$, we used the manufacturer's specified CCD response function (or equivalently the quantum efficiency divided by the wavelength) and multiplied by the atmospheric transmission (Stone & Baldwin 1983). In addition, we have taken care to include the effects of materials in the light paths of the telescopes. The most important changes in the true response function are in the near ultraviolet (i.e., 3000 to 4000 Å); at these wavelengths, layers of glass in the camera lens or covering the CCD window can affect the throughput of the telescope. In addition, aluminum and other mirror coatings can affect the ultimate transmission. Among the observatories in Table 1, these effects are only significant for KAIT (LOSS), which boasts a strong UV CCD response. Figure 1 displays the effective CCD response functions for the observatories listed in Table 1. In Table 2, response characteristics for these CCDs are listed. Column (3) contains the wavelengths of peak efficiency (λ_0), column (4) gives the wavelength range within which the CCDs efficiency is more than 10% of the peak ($\lambda_{10\%}$), and column (5) lists the full width at half maximum sensitivity ($\Delta\lambda$).

For each unfiltered system in Table 2, we have numerically integrated equation (2) using a set of 175 spectrophotometric standard stars from Gunn & Stryker (1983). In Figure 2, we show the synthetic values of $V-W$ for these stars versus the standard colors $B-V$, where the W system illustrated is from BAO. The stellar SEDs result in a simple linear relation between the standard color $B-V$ and the pseudocolors. These theoretically derived relations demonstrate that such transformations are highly linear and have a dispersion of less than 0.05 mag for stars with a color of $-0.2 < B-V < 1.5$. By measuring a star's $B-V$ color, we can use these relations to determine its pseudocolor and, equivalently, its transformation to the W system.

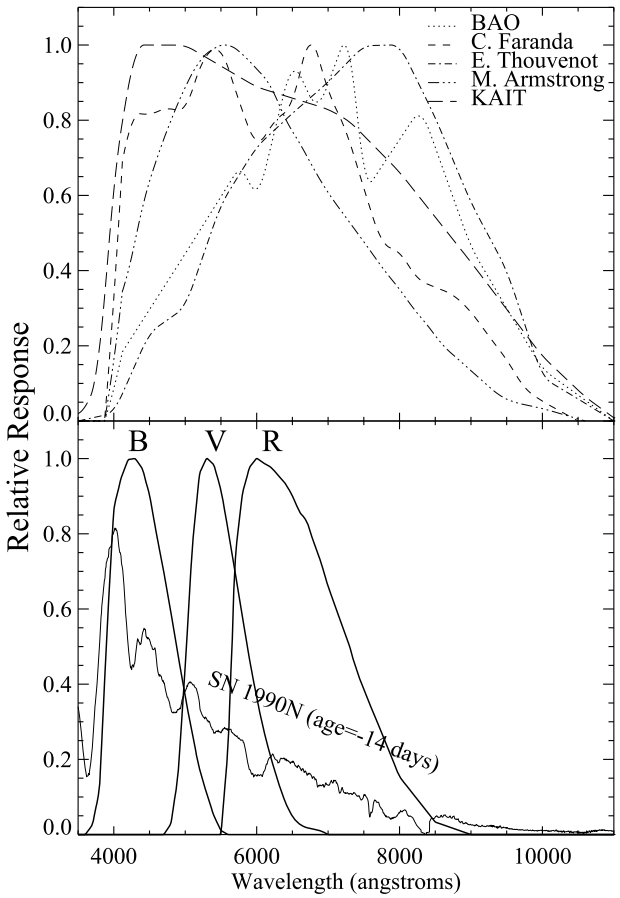

FIG. 1.—Wavelength response functions. For each observer or observatory listed in Table 1, we show the CCD manufacturer's stated response function multiplied by the atmospheric transmission, including effects of glass and mirror transmission. Overplotted for comparison are the Johnson-Cousins B and V response functions. Also shown is the spectrum of SN 1990N at 14 days before B-band maximum light. By accounting for the differences between the SN Ia SED observed by a standard passband and an unfiltered CCD, it is possible to transform an unfiltered CCD observation of an SN Ia to a standard passband.

[8] Zero points are commonly defined to yield $V(\mathrm{Vega}) = W(\mathrm{Vega}) = 0.03$, though this criterion is arbitrary here, since, as will be seen, the transformations are independent of the choice of passband zero points.

TABLE 2

STELLAR UNFILTERED TRANSFORMATIONS

Observer (1)	CCD (2)	λ_0 (Å) (3)	$\lambda_{10\%}$ (Å) (4)	$\Delta\lambda$ (Å) (5)	C_{VW} (σ) (6)	C_{BW} (σ) (7)
BAO	Texas Instruments TC211	6800	3500–10000	4000	0.40 (0.07)	1.40 (0.07)
KAIT (LOSS)	SITe UV2AR	5000	3000–10000	5500	0.33 (0.10)	1.33 (0.10)
E. Thouvenot	Thomson TH7863	7500	4000–10000	3500	0.40 (0.11)	1.40 (0.11)
M. Armstrong.....	Sony ICX027BL	5500	3700–9000	3500	0.31 (0.07)	1.31 (0.07)
C. Faranda	SBIG ST6	5500	4000–10000	3700	0.51 (0.09)	1.51 (0.09)

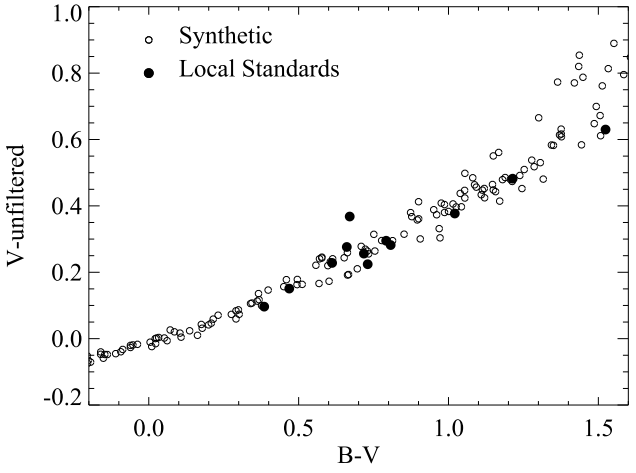

FIG. 2.—For a set of 175 spectrophotometric stars given by Gunn & Stryker (1983), we have calculated synthetic unfiltered CCD magnitudes for the BAO response function of Fig. 1. A comparison of the synthetic $B-V$ colors and the difference between the V and unfiltered magnitudes (*open circles*) shows a well-defined correlation. A similar relation is seen (*filled circles*) by comparing the observed photometry of local standard stars in the fields of SNe. The slope of this correlation defines a transformation between unfiltered and standard passband magnitudes as a function of $B-V$ color.

We can now approximate equation (2) with a simpler expression valid for stars:

$$V-W = C_{VW}(B-V)\,, \tag{3}$$

where C_{VW} is the slope of the linear relation between the standard color and the pseudocolor and we impose the condition that $V-W=0$ when $B-V=0$. While in principle we can derive the values of C_{VW} from the theoretical sensitivity functions of the W passbands and spectrophotometry of stars, the most reliable way to solve for these values is to empirically measure them from the observed magnitudes of LS stars. This method has the advantage that it reduces our reliance on accurately assessing the sensitivity functions of the W systems.

For all the LS stars in the fields of the SNe, we empirically fitted the values of C_{VW} with equation (3) using the instrumental W system magnitudes of the LS stars. In some cases we were able to obtain the W system magnitudes of Landolt (1992) fields. These C_{VW} are given in Table 2 (col. [6]), as are transformation coefficients to B, C_{BW} (col. [7]). Some empirical insight into the response functions of the unfiltered CCD systems can be gained by comparing the values of the coefficients, C_{VW}, with the correlation coefficients between two standard colors. The relations between the standard color $B-V$ and other standard colors calculated from the Gunn & Stryker (1983) spectrophotometric standards are

$$V-I = 0.94(B-V)\,, \tag{4}$$

$$V-R = 0.51(B-V)\,, \tag{5}$$

$$V-V \equiv 0.0(B-V)\,, \tag{6}$$

$$V-B \equiv -1.0(B-V)\,, \tag{7}$$

where the first two relations hold for stars with $B-V<1.3$ mag.

As seen in Table 2, the values of C_{VW} range from 0.3 to 0.5. Comparing equation (3) with equations (4)–(7), we note that the unfiltered CCD response functions have peak efficiency between V and R, although the wavelength regions between B and I are also sampled, as seen in Figure 1 and Table 2. As shown in Figure 2, the theoretical and empirical determinations of C_{VW} are in good agreement. This was true for all W systems in Table 2.

By use of equation (3) (the empirical version of eq. [2]), we have transformed the magnitudes of the LS stars in V (i.e., the standard system) to the W system. Adding these transformed magnitudes to equation (1) yields the magnitude of an SN on the W system.

Unfortunately, early SN magnitudes in these nonstandard systems cannot readily be compared with subsequent observations through standard passbands. Therefore, we seek a transformation of the SN magnitude from the W system to a standard passband system. (An alternative is to transform subsequent SN magnitudes calibrated on standard systems to the W system, but the results would be difficult to evaluate.)

The transformation we need is the inverse (i.e., the negative) of equation (2), except $F_\lambda(\lambda)$ is now the SED of an infant SN Ia. This pseudocolor is equivalent to a cross-filter K-correction between the W and V systems, as expressed by Kim, Goobar, & Perlmutter (1996), except no redshifting of the spectrum is involved (i.e., $z=0$). The appropriate SN Ia spectrum for this calculation is one at a similar age and color as the SN Ia to be transformed. We employed the earliest spectrum of SN 1990N shown in Figure 1 (Leibundgut et al. 1991a) and the earliest spectrum of SN 1994D (Filippenko 1997), both obtained $\sim$14 days before B maximum. These spectra should provide an accurate model of the SED, because their age coincides with the median age of our sample of SNe when they were observed. Because a few of the unfiltered CCD response functions have some minor sensitivity redward of 8200 Å and blueward of 3600 Å, spectra of SN 1994U (Riess et al. 1998b) and SN 1990N (Leibundgut et al. 1991a) at 8 days before maximum were used to augment our description of the early SN Ia SED. This augmentation was included for completeness but has very little effect on the evaluation of equation (2).

Nugent et al. (2000) have found that, to within 0.01 mag, the effects of both extinction and intrinsic color variation on the SN Ia SED can be reproduced by application of a Galactic reddening law (Cardelli, Clayton, & Mathis 1989). The augmented spectra of SN 1990N and SN 1994D were reddened and dereddened using a Galactic reddening law to match the earliest $B-V$ color measurement of each SN Ia listed in Table 3 (col. [2]). In all cases, the earliest color measurement occurred 8 to 12 days before maximum light.

Analysis of the early colors of SNe 1990N (Leibundgut et al. 1991a), 1994ae (Riess et al. 1999b), 1994D (Richmond et al. 1995), 1992bc (Hamuy et al. 1996a), 1997br (Li et al. 1999), 1995bd (Riess et al. 1999b), and 1998aq demonstrates that SNe Ia evolve, on average, by less than 0.05 mag in $B-V$ between 10 to 14 days before B maximum. We conservatively adopt a statistical uncertainty of 1 $\sigma=0.10$ mag for the individual $B-V$ color of a young SN Ia. If the SED of an SN Ia undergoes a dramatic (and unexpected) change between 16–18 days and 14 days before B maximum, a larger error could occur. However, in § 4.2 we demonstrate that this potential systematic error does not affect our analysis. The uncertainties resulting from intrinsic variation in the early SN Ia SEDs are calculated from the dispersion of a set of 12 SN Ia spectra in the range of 8 to 14 days before B maximum.

TABLE 3

SN Ia TRANSFORMATIONS

		THEORETICAL		EMPIRICAL	
SN Ia (1)	EARLY $B-V$ (σ) (2)	$W-V$ (σ) (3)	$W-B$ (σ) (4)	$W-V$ (σ) (5)	$W-B$ (σ) (6)
SN 1996by.....	0.46 (0.03)	−0.13 (0.11)	−0.58 (0.11)	−0.18 (0.04)	−0.64 (0.11)
SN 1996bv.....	0.20 (0.03)	−0.02 (0.09)	−0.21 (0.10)	−0.08 (0.04)	−0.28 (0.10)
SN 1997bq.....	0.04 (0.03)	0.00 (0.08)	0.04 (0.11)	−0.02 (0.02)	−0.06 (0.10)
SN 1998dh.....	0.18 (0.03)	0.07 (0.07)	−0.11 (0.10)	−0.06 (0.04)	−0.25 (0.11)
SN 1998ef.....	0.10 (0.03)	0.06 (0.07)	−0.04 (0.12)	−0.03 (0.03)	−0.13 (0.11)
SN 1998bu.....	0.28 (0.03)	−0.02 (0.09)	−0.21 (0.11)	−0.14 (0.04)	−0.42 (0.11)
SN 1998aq.....	−0.18 (0.03)	0.02 (0.05)	0.20 (0.11)	0.06 (0.03)	0.24 (0.11)
SN 1990N	0.05 (0.03)	0.05 (0.10)	0.00 (0.11)	−0.03 (0.04)	−0.08 (0.10)

Because of the breadth of the unfiltered response functions, we can reasonably transform the data to either the B, V, or R passband systems. The better the match between the filtered and unfiltered response functions, the less we must rely on the accuracy of the transformation. If there is little overlap between the filtered and unfiltered response functions, the pseudocolor becomes similar to a "conventional" color. As seen in Figure 1, the V and R passbands are the closest match to most of the unfiltered response functions. Yet there is a strong historical precedent for measuring rise times relative to B maximum. In addition, for comparison with the rise time measured at high redshift, transforming to the B passband is desirable (Goldhaber et al. 1999; Goldhaber 1998; Groom 1998; Nugent 1998; Riess et al. 1999b). For these reasons, we have chosen to transform the data to both B and V. The greater uncertainty in the B transformation is included in the individual photometric uncertainties. The values and uncertainties in the theoretical pseudocolors $W-V$ and $W-B$ are listed in Table 3 (cols. [3] and [4], respectively). Combining these with equation (1) yields the SNe magnitudes on the standard system. We note that the B and V rise-time measurements will not be independent.

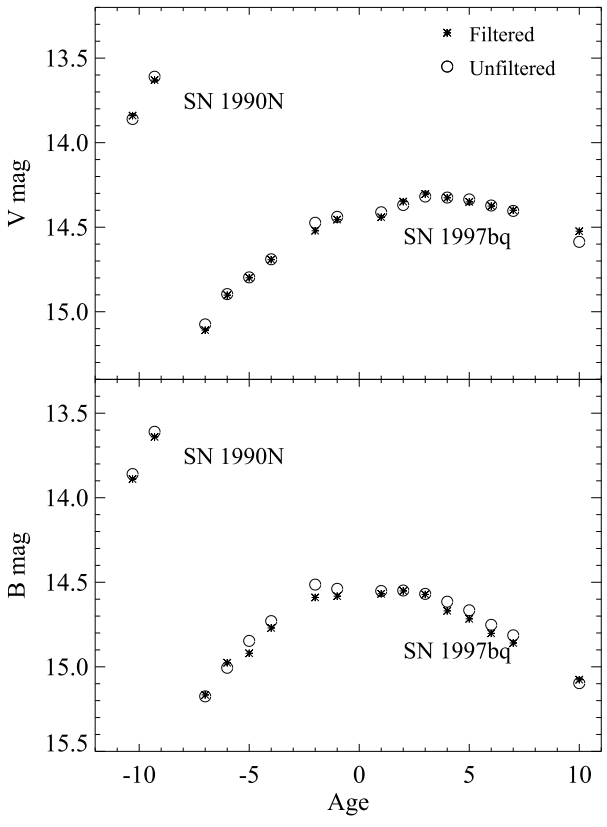

FIG. 3.—Comparison of B and V SN Ia magnitudes observed through standard passbands and transformed to standard passbands using unfiltered CCD observations and the theoretical transformation method. For both SN 1990N and SN 1997bq, the agreement between the standard and transformed magnitudes is excellent, with a relative dispersion of 0.03 and 0.04 mag in V and B, respectively.

An alternate method to transform the unfiltered SN Ia magnitudes to a standard system is to employ the same empirical transformation previously used for stellar SEDs, equation (3), which only depends on the $B-V$ color of the SED. It is well known that the SED of an SN Ia is extremely nonstellar over the vast majority of its observed lifetime (see Filippenko 1997 for a review). However, at very early times the SED of an SN Ia can be photometrically approximated by a thermal continuum (see Fig. 1), making the use of a transformation derived for stars plausible. (It is likely that this thermal continuum is even more dominant when the SNe Ia are younger than the earliest spectral observations.) We used equation (3) and the values of C_{VW} in Table 2 to derive SN Ia pseudocolors,

$$W-V = -C_{VW}(B-V)\,, \tag{8}$$

using the earliest measurements of the SN $B-V$ colors in Table 2. These empirical SN pseudocolors are listed in Table 3 (cols. [5] and [6]). The empirical and theoretical pseudocolors are in good agreement with a relative dispersion of 0.08 and 0.11 mag in V and B, respectively.

The advantage of using these completely empirical transformations is that they do not require explicit knowledge of the unfiltered response functions. The advantage of using the theoretical SN pseudocolors is that we avoid assuming that at very early times SN Ia SEDs are thermal. For the following analysis, we will consider SN transformations derived from both empirical and theoretical pseudocolors. As seen in Table 3 and in §§ 3 and 4, the excellent agreement between the results derived from the two methods suggests that both methods are valid to better than ~ 0.1 mag.

For the unfiltered observations with higher signal-to-noise ratios (S/N $\geq$ 20), the dominant source of uncertainty in the transformed standard magnitudes is the uncertainty in the determination of the SN pseudocolor listed in Table 3. For the observations with lower signal-to-noise ratios (S/N $\leq$ 10), the uncertainty is dominated by the statistics of the measured flux of the SNe.

We have performed a powerful cross-check of the transformation of unfiltered SN Ia magnitudes to a standard passband system by comparing the results with independent, coeval magnitude measurements in standard passbands. We compared B and V magnitudes for SN 1990N at 11 and 12 days before B maximum measured by Lira et al. (1998) with those transformed to B and V, using concurrent unfiltered observations of E. Thouvenot. The mean difference was 0.03 and 0.01 mag for V and B, respectively (see Fig. 3).

An even more powerful test was performed by comparing complete B and V passband light curves of SN 1997bq with B and V light curves transformed from unfiltered measurements obtained by BAO. In this case, it was necessary to use the theoretical SN Ia pseudocolors derived from SNe spectra at appropriate ages, since the assumption that the SN Ia SED matches a thermal spectrum will obviously fail at later times. The uncertainties in transformations at these later ages are smaller because of the increased availability of spectra to model the SED. As seen in Figure 3, the agreement with the measurements employing passbands is excellent, with a dispersion of 0.03 and 0.04 mag in V and B (respectively) for 14 points.

We conclude that we can reliably transform unfiltered CCD SN Ia observations to a standard passband system at a valuable precision of $\sim 5\%$, and we expect that the resulting early measurements of SN Ia magnitudes can yield important constraints on the SN Ia rise-time behavior.

3. RISE CURVE

We first examined the SN Ia rise behavior by subtracting the fitted date and magnitude of maximum from each light curve. The maxima were derived from second-order polynomial fits to data within 5 days of the peak. (This is an iterative procedure.) The individual data points minus the fitted peak magnitudes and dates are listed in Table 4.

The result, as seen in Figure 4, is illuminating. Systematic differences in these prototypical SN Ia light curves are readily visible. Particularly noteworthy is the apparent correlation between the rate of the early rise and the subsequent decline, also noted by Goldhaber (1998). This phenomenon is exemplified by the well-sampled SN 1990N; it

TABLE 4

SN Ia DATA

	B			V		
SN	Age[a]	Magnitude[b]	σ (mag)	Age[c]	Magnitude[d]	σ (mag)
SN 1996by.....	−13.85	3.01	0.23	−15.01	2.97	0.21
	−10.82	1.42	0.16	−11.98	1.38	0.14
	...	...	...	−9.98	0.85	0.03
SN 1994D	−11.71	2.35	0.06	−12.67	2.12	0.05
	−10.86	1.81	0.05	−11.84	1.75	0.04
	−9.90	1.39	0.05	−10.86	1.36	0.04
SN 1997bq.....	−15.67	4.01	0.18	−18.63	4.26	0.16
SN 1998dh.....	−18.70	>4.80	0.30	−20.38	>4.86	0.30
	−14.70	3.01	0.14	−16.38	3.04	0.12
	−10.70	1.24	0.14	−12.38	1.27	0.12
	−9.70	1.09	0.03	−11.38	1.12	0.03
	...	...	...	−10.38	0.85	0.03
SN 1990N	−17.92	3.32	0.15	−19.98	3.33	0.13
	−17.02	2.74	0.15	−19.08	2.75	0.13
	−16.02	2.24	0.15	−18.08	2.25	0.13
	−15.02	1.97	0.15	−17.08	1.98	0.13
	−14.02	1.56	0.15	−16.08	1.57	0.13
	−13.02	1.34	0.15	−15.08	1.35	0.13
	−12.02	1.12	0.15	−14.08	1.13	0.13
	−10.92	0.87	0.15	−12.98	0.87	0.13
	−11.92	1.11	0.03	−13.98	1.12	0.03
	−10.92	0.86	0.03	−12.98	0.91	0.03
	...	...	...	−9.98	0.42	0.03
SN 1998bu.....	−20.74	>6.30	0.30	−22.04	>6.50	0.30
	−16.74	4.65	0.18	−18.04	4.75	0.15
SN 1998aq.....	−20.82	>5.13	0.30	−22.08	>5.25	0.30
	−14.82	2.79	0.16	−16.08	2.88	0.12
	−10.82	1.19	0.05	−12.08	1.28	0.05
	−9.82	0.89	0.04	−11.08	0.98	0.04
	...	...	...	−10.08	0.77	0.03
SN 1998ef.....	−17.02	>4.00	0.30	−18.48	>4.02	0.30
	−13.02	2.32	0.14	−14.48	2.27	0.12
	...	...	...	−10.48	0.80	0.12
SN 1996bv.....	−12.12	1.20	0.22	−14.48	1.49	0.21
SN 1996bo.....	−12.05	1.45	0.10	−13.61	1.64	0.10

[a] Age relative to B maximum in days.
[b] Magnitude relative to B maximum.
[c] Age relative to V maximum in days.
[d] Magnitude relative to V maximum.

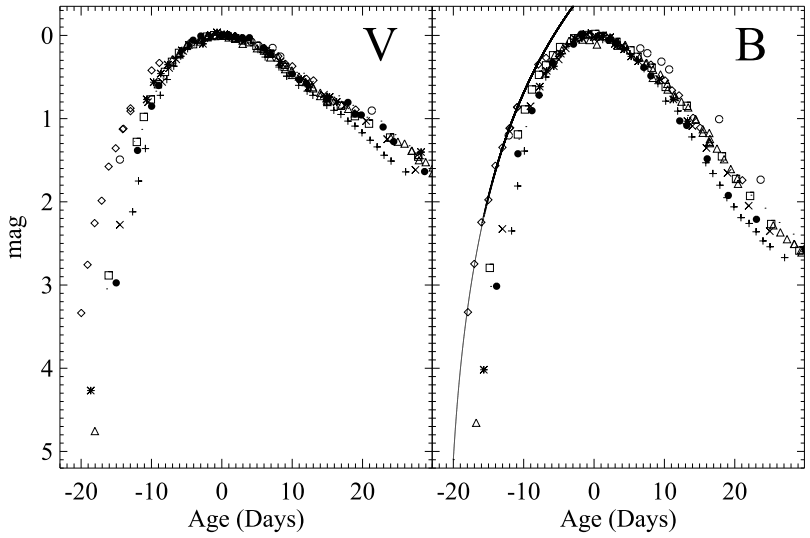

FIG. 4.—*Left*: Observed V-band light curves for 10 SNe Ia including rise-time observations transformed from unfiltered CCD measurements. For each SN Ia, the time and magnitude of the peak has been fitted and subtracted from the data. Significant inhomogeneity is apparent including a strong correlation between the rate of rise and decline to maximum. *Right*: Same as left panel, but using observations and transformations to the B passband. In addition, an empirical model, equation (10), is shown as a fit to the data for SN 1990N.

appears to rise and decline 15% to 20% more slowly than does SN 1994D. The sense of this correlation has been extensively noted by other workers (Phillips 1993; Hamuy et al. 1995, 1996b; Riess, Press, & Kirshner 1995, 1996; Riess et al. 1998a; Tripp 1997, 1998), except these data extend to much earlier ages than were previously explored, leaving little chance that a discontinuity or break from this rule occurs at earlier times. Because it has been previously demonstrated that the SN Ia decline rate is correlated with SN Ia luminosity (Phillips 1993; Hamuy et al. 1995, 1996b; Riess et al. 1995, 1996, 1998a; Tripp 1997, 1998), we may also conclude that brighter SNe Ia rise more slowly and explode longer before maximum than do faint SNe Ia.

These conclusions are only qualitative. Now we proceed to a quantitative exploration of the early SN Ia light curve. To accomplish this we need a quantitative model of the rise-time behavior and its variation.

3.1. *Rise-Time Model*

To estimate the rise time, we need a model of the rising light curve of any SN Ia that can be used to estimate the time of explosion. A very simple and sensible model has been presented by Goldhaber (1998) to fit the early phase of the SN Ia rise: it is motivated by the theoretical representation of an SN Ia shortly after explosion as an expanding fireball. Through a passband system on the Rayleigh-Jeans tail of the nearly thermal SED of a newborn SN Ia, the luminosity of the expanding fireball will be

$$L \propto v^2(t + t_r)^2 T \,, \tag{9}$$

where v is the photospheric velocity, T is the temperature (or the model temperature for a dilute blackbody), t is time relative to maximum, and t_r is the rise time (i.e., the time interval between the explosion and the maximum). In the first few days after explosion, the time since explosion, $t + t_r$, will increase by many factors. This is in contrast to the *relative* stability of the temperature (corroborated by the slow change in SN Ia colors) and the velocity (corroborated by the slower fractional change in the wavelengths of absorption minima; Wells et al. 1994; Patat et al. 1996). Hence at very early times the luminosity should be roughly proportional to the square of the time since explosion:

$$L = \alpha(t + t_r)^2 \,, \tag{10}$$

where α is the "speed" of the rise. (For our empirical model, the speed of the rise is the change in luminosity over a fixed time interval.) Although this model is motivated by theoretical arguments, it is empirically justified by the well-sampled early rise of SN 1990N (see Fig. 4). This model assumes that at the explosion time the luminosity of an SN Ia is zero. In principle, the initial luminosity is that of a white dwarf ($M_B = 10$ to 15 mag), but at the observed speed of the rise, the brightening from zero to a white dwarf luminosity requires less than 1 s.

3.2. *Inhomogeneity*

It is clear from Figure 4 that the rise-time behavior of SNe Ia is considerably inhomogeneous and we cannot expect any single set of parameters (t_r, α) in equation (10) to suffice for our sample. Yet the rise is also likely related to the subsequent shape or decline of the light curve.

A general and economical hypothesis is that the rise parameters for an individual SN Ia are a linear function of the subsequent light-curve shape

$$t_r = RX - t_0 \,, \tag{11}$$

$$\alpha = SX + \alpha_0 \,, \tag{12}$$

where X is any parameter that quantifies the postrise light-curve shape and R and S are linear correlations coefficients between X and the rise time and speed, respectively. Substituting equations (11) and (12) into equation (10) yields a custom rise model for any SN Ia whose individual rise time and speed depends only on the light-curve shape parameter X:

$$L = (SX + \alpha_0)(t + RX - t_0)^2 \,. \tag{13}$$

For a sample of SNe Ia, there are four free parameters: the "fiducial" rise time, t_0, the fiducial speed, α_0, the linear correlation coefficients between X and the rise time, R, and the speed, S.

Two popular methods for quantifying SN Ia light-curve shapes are the decline-rate method (Phillips 1993; Hamuy et al. 1996b) and the multicolor light-curve shape (MLCS) method (Riess et al. 1996, 1998a). The former method employs the parameter $\Delta m_{15}(B)$, the decline in B mag from peak to 15 days hence. Typical SNe Ia have $\Delta m_{15}(B) = 1.1$ mag. The MLCS method correlates the differences between individual light-curve shapes and a fiducial template shape with the differences between individual peak visual luminosities and the fiducial peak luminosity, $\Delta \equiv M_V - M_V$ (fiducial). Jha et al. (1999) and Riess et al. (1998b) adopted M_V(fiducial) $= -19.34$ mag. The values of the parameters $\Delta m_{15}(B)$ and Δ for our sample are given in Table 5.

It is sensible to define the fiducial SN Ia (i.e., $X = 0$) to match the most commonly observed SN Ia, so that the fiducial rise-time parameters will characterize the mode of the population. Because the luminosity calibration of typical SNe Ia is still subject to change, we adopt the simple light curve based criterion $\Delta m_{15}(B) = 1.1$ mag to characterize the fiducial SN Ia. For the purpose of comparing the two light-curve methods, we set M_V(standard) (i.e., $\Delta = 0$) to be the luminosity of an SN Ia with $\Delta m_{15}(B) = 1.1$ mag. With this choice, both methods will be measuring the same fiducial rise time. Using Cepheid calibrations of a set of nearby SNe Ia, Saha et al. (1999) find $M_V = -19.45$ mag for an SN Ia with $\Delta m_{15}(B) = 1.1$ mag.

We tried both methods in our rise model by substituting $X = \Delta$ and $X = \Delta m_{15}(B) - 1.1$ into equation (13). Because the MLCS method derives Δ from a simultaneous fit to all available light curves, we used $X = \Delta$ to model the rise data transformed to both B and V. In contrast, our values of $\Delta m_{15}(B)$ were derived solely from the B light curves (using the parameter definition), so this parameter was only used to model the B-band rise.

TABLE 5

SN Ia Parameters

SN Ia	Δ (σ)[a]	$\Delta m_{15}(B)(\sigma)$	$s(\sigma)$
SN 1996by.....	0.25 (0.05)	1.37 (0.06)	0.85 (0.02)
SN 1996bo.....	0.21 (0.05)	1.22 (0.06)	0.93 (0.02)
SN 1996bv.....	−0.32 (0.07)	0.94 (0.08)	1.14 (0.03)
SN 1997bq.....	0.14 (0.05)	1.23 (0.05)	0.89 (0.02)
SN 1998dh.....	0.14 (0.05)	1.23 (0.05)	0.94 (0.02)
SN 1998ef.....	0.06 (0.05)	1.29 (0.05)	0.92 (0.01)
SN 1998bu.....	0.02 (0.05)	1.15 (0.05)	0.96 (0.01)
SN 1998aq.....	0.10 (0.05)	1.12 (0.05)	0.94 (0.01)
SN 1990N	−0.33 (0.05)	1.03 (0.06)	1.02 (0.02)
SN 1994D	0.39 (0.05)	1.40 (0.05)	0.82 (0.01)

[a] $\Delta = 0$, when $M_v = -19.34$ (Jha et al. 1999).

The most likely values for the free parameters in equation (13) were found by minimizing the χ^2 statistic, the standard measure of the quality of the fit between model and data. We simultaneously fitted all data earlier than 10 days before maximum. After 10 days before maximum our simple rise model fails to describe the light curve (see Fig. 4). As illustrated in Figure 5, the age by which we discontinue the fit does not impact the measured rise time until approximately 8 days before maximum, when the value of χ^2_ν also rises dramatically. By this age it is not surprising that the model would fail: the fractional time since explosion is no longer changing rapidly compared with the velocity and temperature. We have conservatively chosen to fit only data at 10 days before maximum and earlier to avoid biasing the fit by the inadequacies of the model. In § 4, we discuss the relevance of the correlations of the uncertainties in individual observations. All fits yielded values of χ^2 within the expected statistical range. The values of the parameters are given in Table 6.

Although the speed parameter α is useful for modeling the rise, it has little physical meaning. The speed is an unknown function of the photospheric velocity, temperature, and dilution factor. The data do favor the existence of a correlation between the speed of the rise and the light-curve shape parameters, in the sense that brighter and more slowly declining SNe Ia are slower risers (i.e., smaller α). Unfortunately, the simplicity of our model provides no

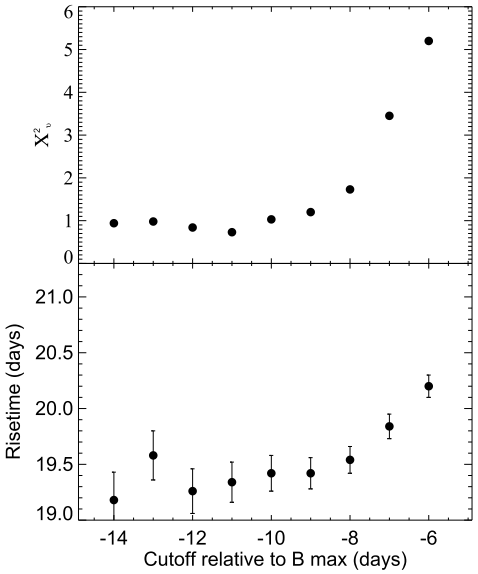

FIG. 5.—Plots of χ^2_ν and rise time vs. the age (relative to B maximum) by which the fit to the rise data is terminated. The fit remains reliable up to ~8 days before B maximum, as evidenced by the acceptable values of χ^2_ν and the relative stability of the rise time. We conservatively use 10 days before maximum as the age by which we terminate the fit.

TABLE 6

SN Ia Rise Time Fits

Method	Band	Fiducial Criterion	χ^2_ν	t_0	R	α_0	S
MLCS.....	B	$M_V = -19.45$	1.0	19.42 ± 0.16	8.0 ± 0.5	0.078 ± 0.002	0.040 ± 0.006
Decline rate.....	B	$\Delta m_{15}(B) = 1.1$	1.3	19.46 ± 0.23	11.7 ± 1.3	0.072 ± 0.003	0.032 ± 0.011
Stretch	B	LT[a]	0.9	19.42 ± 0.19	...	0.071 ± 0.004	...
MLCS.....	V	$M_V = -19.45$	1.4	21.02 ± 0.16	7.7 ± 0.5	0.074 ± 0.002	0.020 ± 0.006

[a] Leibundgut 1989 template.

basis to determine whether the value or variation of the speed has any physical significance.

Of greater physical interest is the fiducial rise time and the correlation between the individual rise time and the light-curve shape. From these parameters, we can determine the explosion time of an SN Ia or, equivalently, the age when observed. To examine these parameters, we converted the χ^2 into a probability density function (pdf; Lupton 1993) and marginalized the pdf over the speed parameters α_0 and S. The resulting confidence intervals for t_0 and R are shown in Figure 6.

Our statistical confidence that the SN Ia rise time is correlated with decline rate and the MLCS method's surrogate parameter for light-curve shape, visual peak luminosity, is very high (16 and 9 σ, respectively).

Both methods concur that the rise time to B maximum of a typical SN Ia (i.e., one with $\Delta m_{15}(B) = 1.1$ mag or $M_V = -19.45$ mag) is 19.5 ± 0.2 days. The MLCS method gives a fiducial rise time to V maximum of 21.1 ± 0.2 days or 1.6 days longer than the B-band rise time. Errors in the peak luminosity calibration of SNe Ia do not affect the rise time but rather the appropriate luminosity for the fiducial rise time.

Using the MLCS method, we find that the brightness of an SN Ia is correlated with the rise time in the sense that for every 0.10 mag increase in visual luminosity, SNe Ia require 0.80 ± 0.05 and 0.77 ± 0.05 days longer to reach maximum in B and V, respectively. We emphasize that this linear relation was determined over a modest range of luminosity ($-19.6 < M_V < -18.9$) and should not be extrapolated beyond this range. Using the decline-rate parameter, we find that slower declining SNe Ia require more time to reach B maximum at the rate of 1.2 ± 0.1 days for a 0.1 mag change in $\Delta m_{15}(B)$. Again, this relation should not be extended beyond the range over which it was derived, $1.39 > \Delta m_{15}(B) > 1.03$. The difference between the B and V fiducial rise times from MLCS is 1.6 days.

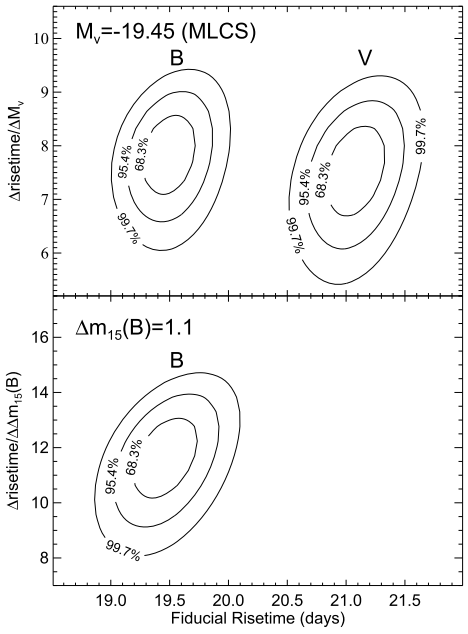

FIG. 6.—Confidence intervals on the rise time parameters. The upper panel shows the likely values of the fiducial (i.e., peak $M_V = -19.45$ mag) rise times to B and V maxima and the correlation between the individual SN Ia B and V rise times and the peak visual luminosity inferred using the MLCS method. The lower panel shows the likely value of the fiducial [i.e., $\Delta m_{15}(B) = 1.1$ mag] B rise time and the relation between the individual B rise time and the decline rate parameter, $\Delta m_{15}(B)$.

3.3. *Light-Curve Normalization*

An alternate method for measuring the rise time of SNe Ia has been proposed by Goldhaber (1998), based on the "stretch" method employed by Perlmutter et al. (1997). The basis of this approach is to first normalize the inhomogeneous light-curve shapes and, by assumption, the rise behavior by dilating the observation times to fit the light curves to a fiducial template light curve. This method is less general than our treatment in § 3.2 because it *assumes* that the rise behavior is correlated with the rest of the light-curve shape in this simple way. Examination of Figure 4 makes this assumption seem plausible; however, the results of § 3.2 indicate that it may be oversimplified. Although the timescale of the rise may be dilated in a similar fashion as the subsequent light curve, the speed of the individual rises also varies. Nevertheless, the reward for employing this method is a reduction of the free parameters of the sample to only two: the rise time (t_0) and the speed (α_0) of the fiducial template.

To find the fiducial rise time with this method, we adopted the template from Leibundgut (1989) as the fiducial template. Because this template light curve has $\Delta m_{15}(B) = 1.1$ mag, the fiducial rise parameters should be directly comparable to the values derived in § 3.2 (assuming the template is otherwise characteristic of typical SNe Ia).

We have employed the stretch method of Perlmutter et al. (1997) by fitting each light curve to the fiducial template. Three parameters and their uncertainties were simultaneously fitted: the epoch of maximum, the peak magnitude, and the stretch factor, s. In all cases, *data 10 or more days before maximum were excluded* from the fit to the light curves so that the rise-time behavior is normalized by the post–rise-time data, independent of the rise. Further, because we do not know a priori the rise-time behavior of the fiducial SN Ia, we cannot compare the rise-time observations to a fiducial template to aid in the determination of the light-curve parameters. In addition, we have not employed data more than 35 days after maximum since the stretch method fails to adequately describe the range of SN Ia behavior at these late times (Perlmutter et al. 1997). The stretch parameters are listed in Table 5.

By applying the fitted parameters to the entire light curve (now including observations earlier than 10 days before maximum), each SN Ia light curve is normalized to a common fiducial template, as shown in Figure 7. The reduction in photometric dispersion of the rise data is impressive. Because the light-curve fits excluded the use of data more than 10 days before maximum, the reduction in dispersion of these data attests to the correlation between the rise and the subsequent light-curve shape.

A lower bound to the typical SN Ia rise time is immediately available from the earliest observations. The earliest SN Ia observation (normalized to the Leibundgut template) is the observation by C. Faranda of SN 1998bu at 18.15 ± 0.25 days before and 4.63 ± 0.16 mag below B maximum. A coeval observation (again as normalized to the Leibundgut template) of SN 1997bq was obtained by BAO at 18.15 ± 0.35 days before and 4.0 ± 0.17 mag below B maximum. From the slope of the rise, we see that at this age

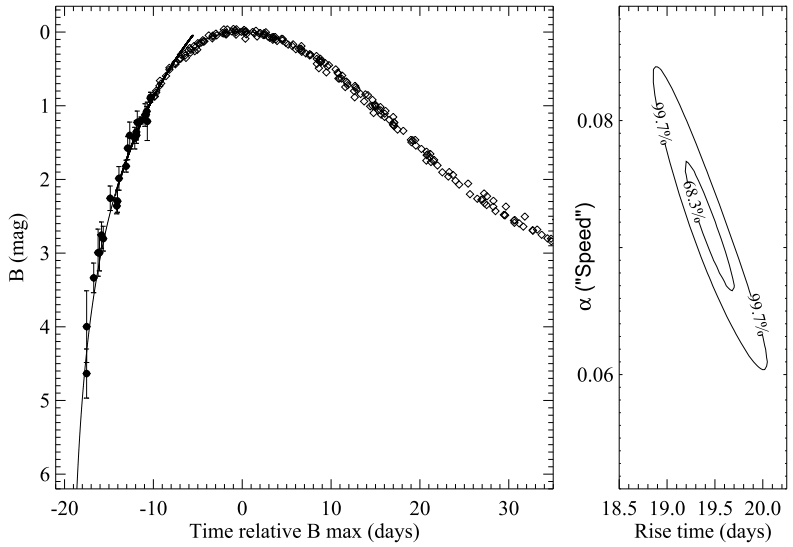

FIG. 7.—Early rise B data normalized by the stretch method and the inferred rise-time parameters. The observation times of the individual SNe Ia are dilated to provide the best fit of the postrise (i.e., after 10 days before maximum) data (*diamonds*) to the Leibundgut (1989) fiducial template. Fitting equation (10) to the rise data (*filled circles*) yields the likely values for the speed of the rise and the rise time to B maximum.

the B luminosity of an SN Ia is increasing 5% every hour. From a weighted average of these two earliest observations, we conclude that the rise time to B maximum (for an SN Ia resembling the Leibundgut template) must be greater than 18.15 ± 0.22 days.

We fitted equation (10) to the normalized rise data to find the fiducial rise time and speed of the template. In accordance with the results in Figure 5, we only fitted data earlier than 10 days before B maximum. To fit the model to the data, we converted the individual age uncertainties of the data points to magnitude uncertainties using the local tangent of the model (i.e., $\sigma_L = 2\alpha\sigma_t$; Press et al. 1992). The fit to the data is shown in the left panel of Figure 7.

The confidence intervals of the parameters (t_r, α) are shown in the right panel of Figure 7. The values of the goodness-of-fit statistic, χ^2_ν, listed in Table 6, show that the rise-time behavior is well modeled by equation (10). The result is that an SN Ia with a light-curve shape similar to the Leibundgut template would explode 19.42 ± 0.19 days before B maximum (although the individual rise times range from 16 to 21 days). This result is derived using the theoretical SN Ia pseudocolors, but the empirical SN Ia pseudocolors give a consistent result with a rise time shorter by 0.18 days.

This result is in excellent agreement with the rise-time value of 19.5 ± 0.2 days to B maximum for typical SNe Ia derived in the previous section.

3.4. *Nondetections*

In addition to the ~ 30 detections of SNe Ia earlier than 10 days before B and V maximum, we have four additional observations of the host galaxies obtained near the time of explosion in which SN light is not present. For these observations, we determined the detection limits empirically by adding artificial stars at a range of brightnesses above and below the approximate detection level. Unfortunately, these upper limits provide negligible additional constraints on the rise behavior; the latest limit is one-half days after the fitted time of explosion, when the SN Ia (SN 1998dh) would be ~ 7 mag below its peak in B or V, but the distance of this object results in a lower limit that is only ~ 4 mag below peak. To detect an SN Ia at this age would require both an SN Ia as near as the Virgo cluster and a telescope that can reach ~ 19 mag in search mode (i.e., with short exposures). Although the upper limits presented here do not add to our constraints on the SN Ia rise behavior, in the future such observations may yield useful results; on good nights, for example, the LOSS images yield detections at ~ 19 mag.

4. BIASES AND SYSTEMATIC ERRORS

In this section, we consider sources of systematic errors that could bias our measurement of the SN Ia rise behavior. Because the stretch method gives consistent results with the method in § 3.2 but is less computationally intensive to implement, we use this method in the following tests of systematic errors.

4.1. *Selection Bias*

A bias in our rise-time measurement can result from an intrinsic dispersion in the rise time of SNe Ia with the same postrise light-curve shape. Although we have already normalized the rise behaviors for the variations in the one-parameter family of light-curve shapes, some dispersion in the rise time might exist for SNe with the same subsequent light-curve shape. Given a variation of rise times, SNe that spend more time above a detection limit before maximum will preferentially be discovered and included in our sample. This would bias the average toward "slow risers" (i.e., long rise times.)

As seen in Table 6, the values of χ^2_ν for the fits to the rising data are all within their expected statistical range, indicating that there is little or no intrinsic dispersion of the rise time after normalizing the light-curve shapes. If no intrinsic dispersion is evident at the resolution of the data, the bias on the measured rise behavior can be neglected. Nevertheless, we can use an additional criterion to select a subsample of SN Ia data from which we can infer the unbiased rise time. This criterion only includes SNe that were discovered

later than 10 days before maximum. This condition guarantees that the rise time of any SN Ia did not influence its discovery and hence its inclusion into our unbiased subsample. The SNe Ia in our full sample that fail this criterion are SNe 1990N, 1994D, and 1998aq.[9]

Even SNe Ia that were discovered later than 10 days before maximum, yet were detected in prediscovery images, must be scrutinized. To insure an unbiased measurement of the rise time, it is necessary to measure all prediscovery observations of the host galaxy, regardless of whether SN light is clearly present. One of our earliest SN detections, that provided by C. Faranda of SN 1998bu, was posted on the amateur SN search network VSNET (and brought to our attention by P. Meikle). Yet it may be that this report exists *only because the SN was evident* in the observation. Had the SN not been present in the observation, the null detection might not have been reported and this object would not have been included in our sample. The selection of an early observation because of the presence of SN light can lead to a bias toward slow and long risers (for a given light-curve shape). Therefore, we conservatively discarded SN 1998bu when accumulating our unbiased sample.

What remains in our unbiased sample are only the SNe discovered by LOSS and BAO: SNe 1996bo, 1996bv, 1996by, 1997bq, 1998dh, and 1998ef. All of these objects were discovered later than 10 days after B maximum, and all prediscovery images of the host galaxy were available for measurement without regard to the presence or absence of SN light. From such data, we can insure that our measurement of the rise behavior is unbiased.

The lower precision results from the unbiased data set are highly consistent with the results from the complete sample. We find a rise time to B maximum of 19.62 ± 0.40 days, in good agreement with the value of 19.42 ± 0.19 from the full set of SNe Ia data. We conclude that no bias toward longer rise times is evident in the full sample.

4.2. *Color of a Newborn SN Ia*

Systematic errors in the unfiltered SN Ia transformations could arise from a significant failure of our assumption that the $B-V$ colors do not evolve between our earliest observations at 16 to 18 days before maximum (~ 2 days after explosion) and 14 days before maximum, by which time SN Ia $B-V$ colors have been observed (Leibundgut et al. 1991a; Richmond et al. 1995; Riess et al. 1999b; Hamuy et al. 1996a). We can remove the influence of this assumption in numerous ways.

One method is to transform some of the unfiltered observations to the R passband. Over the range $0.0 < B-V < 1.5$, the coefficient of the linear transformation is $C_{RW} = 0.0 \pm 0.05$ mag for E. Thouvenot's CCD. For any value of $B-V$ of a young SN Ia within this range, the transformation to R is independent of $B-V$. We inferred the explosion time from the data of SN 1990N transformed to R and measured the time interval to B maximum. (This method assumes that the time of explosion can be inferred equivalently from observations in different passbands.) The resulting rise time differed by less than 0.05 days, with the value inferred from the transformations to B.

We also refitted the B-band rise time using only data between 10 and 14 days before B maximum. The earliest observations of SN Ia colors are static over this range in age (Leibundgut et al. 1991a; Riess et al. 1999b; Richmond et al. 1995; Hamuy et al. 1996a; Li et al. 1999). Normalized to the Supernova Cosmology Project B template, data between 10 and 14 days before maximum gave a rise time of 19.00 ± 0.52 days, in reasonable agreement with the full data set result of 19.42 ± 0.18 days.

Finally, an unexpected change in the young SN Ia SED or $B-V$ color would have a much larger impact on data transformed to B than those transformed to V. The reason is that the V band is a better match to the unfiltered CCDs, and so the transformation depends less on the form of the SN SED. A systematic difference between the explosion time inferred from transformations to B and V would indicate an unaccounted for change in the SN Ia SED. However, the measured difference between the rise times to B and V maxima from MLCS of 1.6 days is in excellent agreement with the average difference in the times of B and V maxima of 1.64 days. Therefore, the difference in the explosion time inferred from the B and V transformations is less than 0.1 days and shows no evidence of a significant change in the early SN Ia SED.

4.3. *Other*

Another source of potential error arises from the correlation of errors among individual rise-time observations. Specifically, all individual measurements of the same supernova would be expected to share some sources of error. These include the determination of the stellar and supernova pseudocolors and the light-curve fit parameters. While it is possible to account for these correlations, an examination of our observations suggests a straightforward way to minimize the effects of error correlations. Each SN Ia in our set has only one or two detections at early times, with one exception: SN 1990N has a total of 12 observations at 10 distinct ages. By removing SN 1990N from our set, we can remove the dominant source of covariance between observations in our sample. This decreased the rise time by 0.3 days.

5. DISCUSSION

Using a set of the earliest detections of low-redshift SNe Ia, we have made a precise measurement of the rise time of SNe Ia. The low-redshift observations indicate that the rate at which SNe Ia rise and decline is highly correlated.

The rise time to B maximum for a typical SN Ia is 19.5 ± 0.2 days, where "typical" is defined as having a peak of $M_V = -19.45$ mag, $\Delta m_{15}(B) = 1.1$ mag, or a B light curve, which resembles the Leibundgut (1989) template. Brighter and slower declining SNe Ia have a longer rise time

[9] However, an argument can be made that SNe Ia in the three major nearby clusters would be discovered at early phases, regardless of their rise time. SN 1990N and SN 1994D both occurred in the Virgo cluster, the former found by amateur astronomers and the latter by a professional search. The Virgo cluster is a major target of amateur and professional supernova searchers and is monitored with high frequency. In the spring of 1989, a group of amateur astronomers initiated the "Virgo Project" to systematically search for SNe in Virgo (Starburst Newsletter 20 from VSNET). This high frequency of monitoring should result in the discovery of nearly all typical SNe Ia, independent of their rise time. The same conclusion may be appropriate for SN 1998aq, which occurred in the Ursa Major cluster. Nevertheless, it is wise to temporarily discard these objects to be sure that our subsample will yield an unbiased estimate of the rise time.

at the rate of 0.80 ± 0.05 days per 0.10 mag in peak luminosity and 1.17 ± 0.13 days per 0.10 mag in $\Delta m_{15}(B)$. Most SNe Ia [i.e., with $-19.10 > M_V > -19.65$ and $0.95 \leq \Delta m_{15}(B) \leq 1.40$] range in their rise time to B maximum by 16 to 21 days, depending on their specific light-curve shape or width.

We have not considered SNe Ia that are beyond this range for the reasons discussed in § 2.1. However, we have verified that the conclusions presented here do extend to highly subluminous SNe Ia, using early observations of SN 1998de [$\Delta m_{15}(B) = 1.96$ mag], a veritable twin to SN 1991bg (Modjaz et al. 2000).

Our observations are not highly consistent with less precise measurements of the SN Ia rise behavior by Vacca & Leibundgut (1996). They find the rise time to B maximum for SN 1994D [$\Delta m_{15}(B) = 1.32$ mag] to be 17.6 ± 0.5 days, as compared to 15.5 ± 0.5 days found by fitting equation (10) directly to the B data of SN 1994D. This difference is not surprising since Vacca & Leibundgut adopted a very different empirical model (a Gaussian multiplied by an exponential) to fit the rising light curve. The relatively late start of the light curve of SN 1994D could result in large changes in the rise time for different methods used to extrapolate to the time of explosion. An individual B rise-time measurement of 21.4 ± 0.3 days for SN 1990N is somewhat larger than a "loose" upper limit of 20 days estimated by Leibundgut et al. (1991a) using an expanding photosphere approach. Our characteristic SN Ia rise time to B maximum of 19.5 days is significantly longer than the first indications by Barbon, Ciatti, & Rosino (1973) of 15 ± 2 days. Interestingly, our results are in surprisingly good agreement with those of Pskovskii (1984), who found that typical SNe Ia have a rise time of 19 to 20 days and that an 0.1 mag increase in the peak blue luminosity is accompanied by a ~ 0.4 days increase in the rise time.

As noted by Vacca & Leibundgut (1996), we find that most theoretical models of SNe Ia predict significantly shorter rise times than we find. A series of model calculations by Höflich & Khokhlov (1996) generally give rise times to visual maximum of 9 to 16 days, with an average value of about 14 days for single white dwarf progenitors. These models encompass a variety of explosion scenarios: detonations, deflagrations, delayed detonations, pulsations, and helium detonations. The same difference is seen in model calculations by Pinto & Eastman (2000).

Within a family of models, the predicted correlation between luminosity and rise time is opposite of what is observed. Leibundgut & Pinto (1992) calculated a series of classical deflagration as well as delayed detonation models and found that "All models show the trend of decreasing luminosity for longer rise times." The same difference with the observations is true of the models by Höflich & Khokhlov (1996).

The double-degenerate models of Höflich & Khokhlov (1996) (modeled as a detonation within a thick envelope formed by a tidally disrupted companion) can adequately reproduce the observed rise times. These models yield rise times to V maximum of 19.5 to 21.8 days, in good agreement with our fiducial V rise time of 21 days. This consistency could be seen as a reason to favor this candidate as the progenitor system of SNe Ia. However, the double-degenerate models with the longest rise times develop into the dimmest SNe, a trend in poor accordance with our findings.

If these models are otherwise accurate, we concur with the conclusion made by Vacca & Leibundgut (1996) that the model atmospheric opacity has been significantly underestimated. Past work suggests that deficient line lists may be the culprit. By increasing the number of lines from 500 to 100,000, the rise time for models by Harkness (1991) increased by 8 days. More atomic data are needed to determine whether the discrepancy between models and observations can be resolved. Ideally the rise-time predictions of different models could be used to discriminate between proposed explosion mechanisms and progenitor types. Unfortunately, deficiencies of the current suite of models makes it difficult to assess which model characteristics are favored at the present time.

Recently, Höflich et al. (1998) have found that reducing the carbon-to-oxygen ratio of the white dwarf progenitor from the previously assumed value of unity increases the rise time to values that appear to be a better match to the measurements reported here. These models have the advantage that SNe Ia with longer rise times reach brighter peak luminosities, in agreement with what our findings reveal. However, these models do not appear to match the well-known trend between peak luminosity and decline rate.

Assuming that the rise time to B maximum is a good approximation of the bolometric rise time as found by Vacca & Leibundgut (1996), we can use theoretical scaling laws from Nugent et al. (1995) to assess the peak absolute luminosity of SNe Ia. Using the rise time to measure the rate of energy deposition from the radioactive decay of ^{56}Ni and ^{56}Co with an SN Ia bolometric correction to B band of 0.2 mag (Höflich & Khokhlov 1996), we find $M_B = -19.4 \pm 0.3$ mag. An alternate method using the rise time to measure the size of the dilute expanding photosphere at maximum gives $M_B = -19.8 \pm 0.3$ mag. The two methods are in rough agreement with each other, as well as with current Cepheid-based calibrations of the SN Ia peak luminosity of $M_B = -19.45 \pm 0.10$ from Saha et al. (1999). However, the qualitative differences between the observed and theoretically predicted rise times cast doubt on the integrity of even semitheoretical routes to the luminosity calibration of SNe Ia.

We emphasize that an accurate determination of the rise time is not the limiting challenge for a theoretical determination of the fiducial peak SN Ia luminosity. Within a single parameterized model, Leibundgut & Pinto (1992) find that a change in the rise time by 1 day results in a change in peak luminosity by 3% (again, in the opposite direction to the observations reported here). Yet, for a given rise time, they find that different models support a 50% range in peak luminosity.

In the future, theoretical models need to be sharpened and reworked to match the increasingly precise observational constraints on the behavior of SNe Ia. We hope that the characterization of the fiducial value and variation of the SN Ia rise time presented here can serve as a guide in the quest to develop a satisfactory theoretical understanding of SNe Ia.

We wish to thank Ed Moran, Peter Meikle, Peter Nugent, Gerson Goldhaber, Saul Perlmutter, Don Groom, Robert Kirshner, Peter Garnavich, Saurabh Jha, Nick Suntzeff, and Doug Leonard for helpful discussions. The work at the University of California, Berkeley, was supported by the Miller Institute for Basic Research in Science,

by NSF grant AST 94-17213, and by grant GO-7505 from the Space Telescope Science Institute, which is operated by the Association of Universities for Research in Astronomy, Inc., under NASA contract NAS 5-26555. We are also grateful to the Sylvia and Jim Katzman Foundation, Autoscope Corporation, the National Science Foundation, Photometrics, Ltd., Sun Microsystems, Inc., and the University of California for assistance with the construction and support of KAIT at Lick Observatory.

REFERENCES

Armstrong, M., et al. 1998, IAU Circ. 6497
Arnett, W. D. 1969, ApJ, 157, 1369
———. 1982, ApJ, 253, 785
Arnett, W. D., Branch, D., & Wheeler, J. C. 1985, Nature, 314, 337
Barbon, R., Ciatti, F., & Rosino, L. 1973, A&A, 25, 65
Barbon, R., Ciatti, F., Rosino, L., Ortolani, S., & Rafanelli, P. 1982, A&A, 116, 43
Branch, D., Fisher, A., & Nugent, P. 1993, AJ, 106, 2383
Cardelli, J. A., Clayton, G. C., & Mathis, J. S. 1989, ApJ, 345, 245
Colgate, S. A., & McKee, C. 1969, ApJ, 157, 623
Filippenko, A. V. 1997, ARA&A, 35, 309
Goldhaber, G. 1998, BAAS, 193, 47.13
Goldhaber, G., et al. 1999, in preparation
Groom, D. E. 1998, BAAS, 193, 111.02
Gunn, J. E., & Stryker, L. L. 1983, ApJS, 52, 121
Hamuy, M., Phillips, M. M., Maza, J., Suntzeff, N. B., Schommer, R. A., & Avilés, R. 1995, AJ, 109, 1
Hamuy, M., Phillips, M. M., Maza, J., Wischnjewsky, M., Uomoto, A., Landolt, A. U., & Khatwani, R. 1991, AJ, 102, 208
Hamuy, M., et al. 1996a, AJ, 112, 2408
Hamuy, M., Phillips, M. M., Suntzeff, N. B., Schommer, R. A., Maza, J., & Avilés, R. 1996b, AJ, 112, 2438
Harkness, R. P. 1991, in SN 1987A and Other Supernovae, ed. I. J. Danziger & K. Kjær (Garching: ESO)
Ho, W., et al. 1999, PASP, submitted
Höflich, P., & Khokhlov, A. M. 1996, ApJ, 457, 500
Höflich, P., Khokhlov, A. M., & Müller, E. 1992, A&A, 259, 549
Höflich, P., Wheeler, J. C., & Thielemann, F. K. 1998, ApJ, 495, 617
Hoyle, F., & Fowler, W. A. 1960, ApJ, 132, 565
Jha, S., et al. 1999, ApJS, in press
Kim, A., Goobar, A., & Perlmutter, S. 1996, PASP, 108, 190
Landolt, A. U. 1992, AJ, 104, 340
Leibundgut, B. 1989, Ph.D. thesis, Univ. Basel
Leibundgut, B., Kirshner, R. P., Filippenko, A. V., Shields, J. C., Foltz, C. B., Phillips, M. M., & Sonneborn, G. 1991a, ApJ, 371, L23
Leibundgut, B., & Pinto, P. A. 1992, ApJ, 401, 49
Leibundgut, B., Tammann, G. A., Cadonau, R., & Cerrito, D. 1991b, A&AS, 89, 537
Li, W. D., Qiu, Y. L., Qiao, Q. Y., Ma, J., Hu, J. Y., & Wang, L. 1996, IAU Circ. 6379
Li, W. D., et al. 1999, AJ, 117, 2709
Lira, P., et al. 1998, AJ, 115, 234
Lupton, R. 1993, Statistics in Theory and Practice (Princeton: Princeton Univ. Press)
Marvin, H., & Perlmutter, S. 1989, IAU Circ. 4727
Maury, A., et al. 1990, IAU Circ. 5039
Meikle, P., & Hernandez, M. 1999, Mem. Soc. Astron. Italian, in press
Modjaz, M., et al. 2000, in preparation
Nugent, P. 1998, BAAS, 193, 47.12
Nugent, P., Branch, D., Baron, E., Fisher, A., & Vaughan, T. 1995, Phys. Rev. Lett., 75, 394 (erratum 75, 1874)
Nugent, P., et al. 2000, in preparation
Patat, F., Benetti, S., Cappellaro, E., Danziger, I. J., Della Valle, M., Mazzali, P. A., & Turatto, M. 1996, MNRAS, 278, 111
Perlmutter, S., et al. 1997, ApJ, 483, 565
Phillips, M. M. 1993, ApJ, 413, L105
Pinto, P. A., & Eastman, R. 2000, ApJ, submitted
Press, W. H., Teukolsky, S. A., Vetterling, W. T., & Flannery, B. P. 1992, Numerical Recipes in FORTRAN (2d ed.; Cambridge: Cambridge Univ. Press)
Pskovskii, Y. 1984, Soviet Astron., 28, 658
Richmond, M. W., Treffers, R. R., & Filippenko, A. V. 1993, PASP, 105, 1164
Richmond, M. W., et al. 1995, AJ, 109, 2121
Riess, A. G., et al. 1998a, AJ, 116, 1009
Riess, A. G., Filippenk., A. V., Li, W., & Schmidt, B. P. 1999a, AJ, 118
Riess, A. G., et al. 1999b, AJ, 117, 707
Riess, A. G., Nugent, P., Filippenko, A. V., Kirshner, R. P., & Perlmutter, S. 1998b, ApJ, 504, 935
Riess, A. G., Press, W. H., & Kirshner, R. P. 1995, ApJ, 438, L17
———. 1996, ApJ, 473, 88
Saha, A., Sandage, A., Tammann, G. A., Labhardt, T. L., Macchetto, F. D., & Panagia, N. 1999, ApJ, 522, 802
Schmidt, B. P., et al. 1998, ApJ, 507, 46
Stone, R. P. S., & Baldwin, J. A. 1983, MNRAS, 204, 347
Treffers, R. R., Peng, C. Y., Filippenko, A. V., Richmond, M. W., Barth, A. J., & Gilbert, A. M. 1997, IAU Circ. 6627
Tripp, R. 1997, A&A, 325, 871
———. 1998, A&A, 331, 815
Vacca, W. D., & Leibundgut, B. 1996, ApJ, 471, L37
Van Dyk, S. D., Treffers, R. R., Richmond, M. W., Filippenko, A. V., & Paik, Y. B. 1994, IAU Circ. 6105
Wells, L. A., et al. 1994, AJ, 108, 2233